Air-Coupled Nondestructive Evaluation Using Micromachined Ultrasonic Transducers

Sean T. Hansen, Benjamin J. Mossawir, A. Sanli Ergun, F. Levent Degertekin, and Butrus T. Khuri-Yakub

Edward L. Ginzton Laboratory
Stanford University
Stanford, CA 94305-4085

Abstract— **Nondestructive evaluation techniques which use conventional piezoelectric transducers typically require liquid coupling fluids to improve the impedance mismatch between piezoelectric materials and air. Air-coupled ultrasonic systems can eliminate this requirement if the dynamic range of the system is large enough such that the losses at the air-solid interfaces are tolerable. Capacitive micromachined ultrasonic transducers (cMUTs) have been shown to have more than 100 dB dynamic range when used in bistatic transmission mode. This dynamic range, along with the ability to transmit ultrasound efficiently into air, makes cMUTs ideally suited for air-coupled nondestructive evaluation applications. These transducers can be used either in through transmission experiments at normal incidence to the sample or to excite and detect guided waves in aluminum and composite plates.**

In this paper, we present results of a pitch-catch transmission system using cMUTs that achieves a dynamic range in excess of 100 dB. The pair of transducers is modeled with an equivalent electrical circuit which predicts the transmission system's insertion loss and dynamic range. We also demonstrate the feasibility of Lamb wave defect detection for one-sided nondestructive evaluation applications. A pair of cMUTs excites and detects the s_0 mode in a 1.2 mm-thick aluminum plate with a received signal-to-noise ratio of 28 dB without signal averaging.

Introduction

Many capacitive micromachined ultrasonic transducers (cMUTs) have been developed for efficient excitation and detection of ultrasound in air [1], [2]. Although such a system may efficiently transfer energy to the air, signal losses at the air-solid interfaces remain. Therefore, a system with a large dynamic range is still necessary for defect detection in the sample. Figure 1 shows the structure of a single membrane of a cMUT. A single element consists of a 50 μm-radius, 1 μm-thick metalized silicon-nitride membrane suspended above a silicon substrate. Approximately

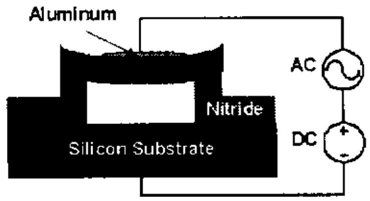

Fig. 1. Schematic cross-section of a single cMUT membrane

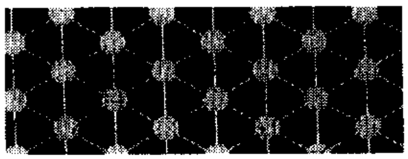

Fig. 2. Magnified view of cMUT transducer with membrane radii of 50 μm

12,000 such membranes are electrically connected in parallel to form a 1 cm^2 transducer, a section of which is shown in Fig. 2. Application of an alternating signal superimposed on a DC bias voltage moves the membrane and generates ultrasound in air. Reception of ultrasonic waves is analogous to generation, as movement of the membrane varies the charge between the capacitor plates formed by the membrane and substrate. The resulting transducer resonates between 2.3 and 2.5 MHz depending on other process parameters, and is capable of a dynamic range of 100 dB.

Equivalent Circuit Modeling

An equivalent circuit model of the cMUT is useful both for transducer design as well as for examining the characteristics and limitations of a defect detection system. The model in Fig. 3 shows a small-signal equivalent of a cMUT operating in air [3], largely based on analysis by Mason [4]. Quantities on the left side of Fig. 3 represent electrical quantities, while elements on the right side are mechanical quantities. A

0-7803-5722-1/99/$10.00

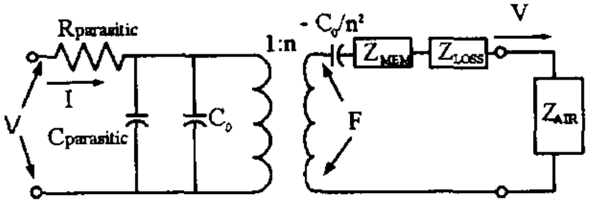

Fig. 3. Equivalent small-signal model of a cMUT membrane

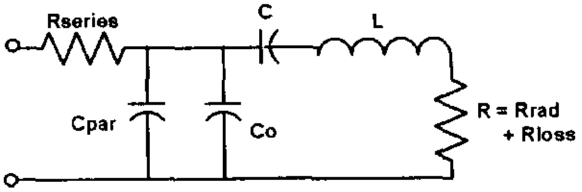

Fig. 4. Electrical circuit model of a transducer

transformer relates electrical quantities of voltage and current to their mechanical analogues, force and velocity. Important mechanical parameters include Z_{air}, the acoustic impedance of air; Z_{loss}, an energy loss mechanism; and Z_{mem}, the impedance of the membrane. The electrical side of the transformer has the parameters C_o, $C_{parasitic}$, and $R_{parasitic}$, which represent device capacitance, parasitic capacitance, and series loss resistance respectively.

If the mechanical impedances are transformed into their equivalent electrical impedances, the transducer model becomes the electrical circuit shown in Fig. 4. In particular, the membrane impedance and negative capacitance terms combine to behave as an inductor, L, and capacitor, C, in series, while the air and loss impedances become a combined resistance, R, capable of power dissipation and radiation. With proper selection of element values, the circuit model in Fig. 4 matches the impedance of the transducer measured on a network analyzer. Both the measurement and model impedances are shown together in Fig. 5 for the circuit element values shown in Table I.

Predictions and Measurements

Once equipped with an accurate circuit model of the transducer, a number of useful system parameters can be extracted. However, the component of loss included in the circuit element, R, is critical for estimating the ultrasonic power that is actually transferred to air, represented by R_{rad}. A measurement of two-way insertion loss of two similar cMUTs in a pitch-catch transmission configuration permits one estimate of the losses within the transducers. Fig. 6 shows a measured two-way insertion loss of 29.3 dB at resonance. Approximately 2.5 dB of this loss is due to electrical impedance mismatch between the signal source, transducers, and the amplifier. The remaining loss mechanisms are internal to the transducers. Fig. 6 also shows that, if we assume transducer losses of 19 times the radiation resistance, the predicted insertion loss near resonance matches the measured results. Comparison of the impedances of cMUTs in air and vacuum suggests that most of the transducer loss is due to viscous damping from air behind the membrane, and finite element simulation suggests that the remaining loss is structural [5]. The particular fabrication procedure used for this pair of cMUTs traps air behind the membrane, leading to more than twice the loss on each transducer than is typically reported for this cMUT design [3]. If the gap between the membrane and substrate were vacuum-sealed, a dramatic reduction in transducer loss would be possible leading to improved dynamic range at the expense of bandwidth.

The most important system consideration for using transducers to inspect a medium with large at-

TABLE I
Values of circuit elements

Symbol	Value
R	$482\,\Omega$
L	$982\,\mu H$
C	$4\,pF$
C_o	$241\,pF$
C_{par}	$111\,pF$
R_{series}	$11\,\Omega$

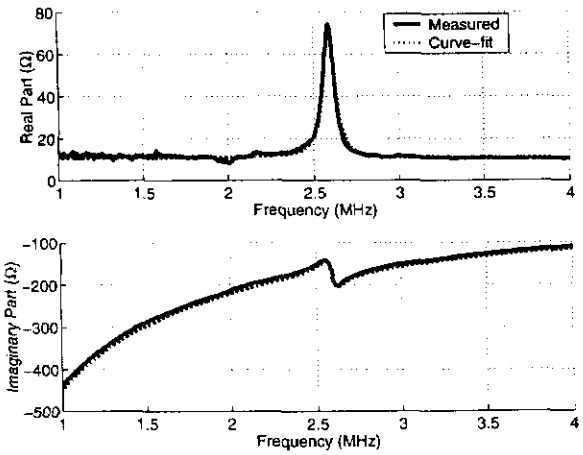

Fig. 5. Measured and modeled impedance of a transducer

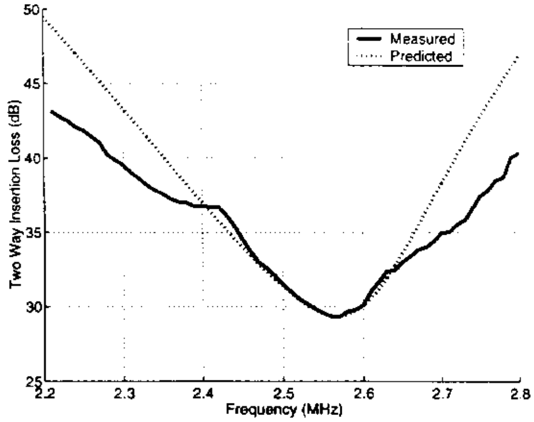

Fig. 6. Predicted and measured two-way insertion loss

tenuation is the system dynamic range. Circuit simulation using a commercially available amplifier with 1.4 $\mathrm{nV}/\sqrt{Hz}$ input-referred noise and a 2.8 MHz noise bandwidth predicts 111 dB dynamic range for the system with an input voltage amplitude of 28 V. Actual measurements using the described system and the simulated transducers demonstrate a 100.3 dB dynamic range. One might expect a slightly lower attainable dynamic range than predicted since electromagnetic interference and imperfect alignment are unknown and cannot be modeled. Nonetheless, a dynamic range of 100 dB is more than sufficient for many air-coupled defect detection and imaging applications. Fig. 7 shows an example of air-coupled ultrasonic transmission through a 3 mm-thick aluminum plate at 2.3 MHz, using a different set of transducers. With a 16 dB received signal-to-noise ratio without averaging, 82 dB of loss due to the aluminum plate, and 5 dB of signal attenuation in air, this system has a total dynamic range of 103 dB.

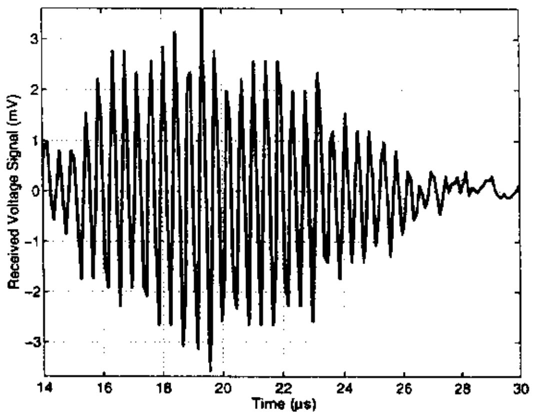

Fig. 7. Received voltage signal through 3 mm-thick aluminum plate (no signal averaging)

Lamb Wave Results

Generation and detection of Lamb waves from air into plates is a promising method for inspecting materials and structures in which only one side of the sample is accessible. Furthermore, the conversion losses in coupling Lamb waves to and from the plate are generally less than for transmission experiments, resulting in improved received signal-to-noise ratios. Proper alignment of the transducers over the sample is critical, however. Fig. 8 shows a schematic representation of the experimental setup.

At a frequency of 2.3 MHz and an aluminum plate thickness of 1.2 mm, an angle of incidence of 5.8° couples the lowest order symmetric mode, s_0, from air into the plate. Multiple reflections of the Lamb wave from both ends of the plate result in echoes that are visible in the received voltage signal shown in Fig. 9. Estimation of the group velocity using the time between echoes confirms that this is indeed the s_0 mode. Another measurement of dynamic range is possible from the received voltage signal. Fig. 10 shows received voltage signal from the Lamb wave, averaged 16 times. With a predicted two-way conversion loss of 61.5 dB, a measured signal-to-noise ratio of 28.4 dB, and 8.7 dB attenuation from air gaps, the dynamic range appears to be 98.6 dB for this set of transducers.

A measured signal-to-noise ratio of 29 dB is sufficient to detect the presence of slight thickness changes in the aluminum plate, representing possible defects. By scanning transducers in a line over a series of milled defects of varying depths, as shown in Fig. 11, one observes the sensitivity of Lamb waves to changes in plate thickness. The defect depths of Fig. 11 are 0.05 mm, 0.10 mm, 0.15 mm, 0.3 mm, and 0.45 mm in a 1.2 mm-thick aluminum plate. Fig. 12 plots the received voltage signal as a function of scanning distance as the defect depth increases. Even a 5% change in the plate thickness alters the propagation conditions for the Lamb waves in the plate, resulting in a noticeable drop in received signal amplitude.

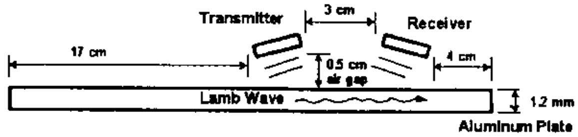

Fig. 8. Measurement configuration for coupling a Lamb wave to and from an aluminum plate

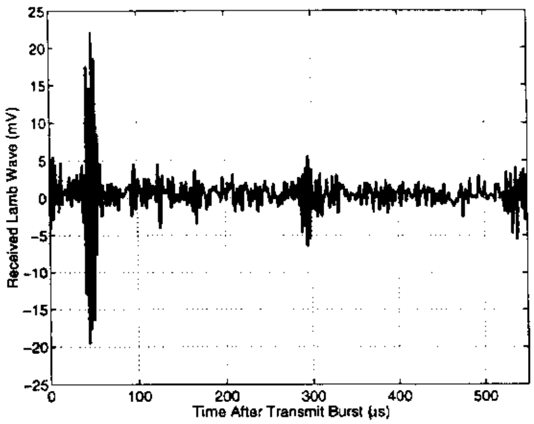

Fig. 9. Received voltage signal showing multiple reflections of s_0 mode Lamb wave

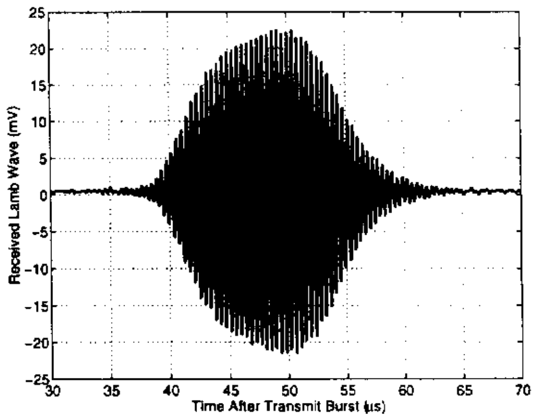

Fig. 10. Received voltage signal from air-coupled s_0 Lamb wave, averaged 16 times

CONCLUSION

Experimental data from transmission experiments demonstrates 103 dB dynamic range without signal averaging. This dynamic range, along with the ability to efficiently transmit ultrasound in air, makes cMUTs ideally suited for air-coupled nondestructive evaluation applications. For rapid one-sided inspection, the transducers may be used to excite and detect Lamb waves in thin plates. Future work includes research and development of broadband cMUTs that do not sacrifice dynamic range for bandwidth. Such transducers can be excited with shorter tone-bursts, improving the temporal resolution of reflections from various depths in pulse-echo inspection.

ACKNOWLEDGMENTS

This work is supported by WPAFB and the U.S. Office of Naval Research.

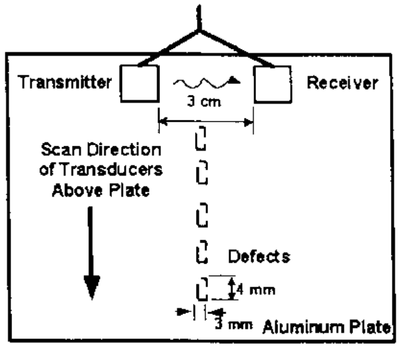

Fig. 11. Configuration for Lamb wave scan over plate

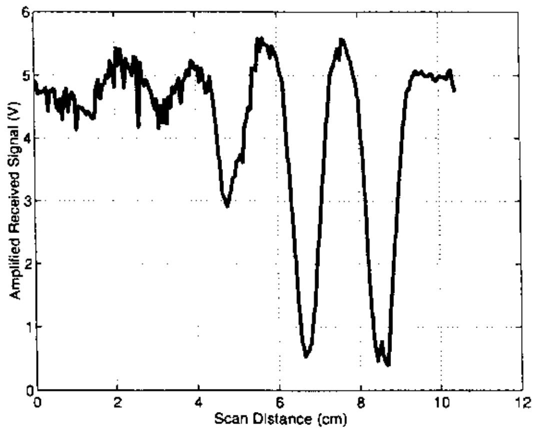

Fig. 12. Received voltage amplitude from Lamb wave scan over plate defects

REFERENCES

[1] M. I. Haller and B. T. Khuri-Yakub, "A surface micromachined electrostatic ultrasonic air transducer," *IEEE Transactions on Ultrasonics, Ferroelectrics, and Frequency Control*, vol. 43, no. 1, pp. 1–6, January 1996.

[2] D. W. Schindel, D. A. Hutchins, L. Zou, and M. Sayer, "The design and characterization of micromachined air-coupled capacitance transducers," *IEEE Transactions on Ultrasonics, Ferroelectrics, and Frequency Control*, vol. 42, no. 1, pp. 42–50, January 1995.

[3] I. Ladabaum, X. C. Jin, H. T. Soh, A. Atalar, and B. T. Khuri-Yakub, "Surface micromachined capacitive ultrasonic transducers," *IEEE Transactions on Ultrasonics, Ferroelectrics, and Frequency Control*, vol. 45, no. 3, pp. 678–690, May 1998.

[4] W. P. Mason, *Electromechanical Transducers and Wave Filters*, Van Nostrand, 1942.

[5] A. Bozkurt, F. L. Degertekin, A. Atalar, and B. T. Khuri-Yakub, "Analytic modeling of loss and cross-coupling in capacitive micromachined ultrasonic transducers," in *Ultrasonics Symposium Proceedings*, Sendia, Japan, October 1998, IEEE Ultrasonics, Ferroelectrics, and Frequency Control Society, pp. 1025–1028.